Photon-counting chip-interleaved iterative PIC detector over atmospheric turbulence channels

Xiaolin Zhou (周小林)*, Yandong Yang (杨彦东), Yufeng Shao (邵宇丰), and Jun Liu (刘 俊)

Department of Communication Science and Engineering, Fudan University, Shanghai 200433, China

**Corresponding author: zhouxiaolin@fudan.edu.cn*

Received April 14, 2012; accepted June 20, 2012; posted online September 28, 2012

A photon-counting-based iterative parallel interference cancellation (PIC) scheme for free-space optical communications in the presence of multiple-access interference, shot noise, background radiation, and turbulence fading is designed. An efficient chip-level iterative equivalent noise estimation algorithm is also derived. Simulation results show that the proposed scheme can achieve a single-user performance, bound with the fast convergence property. More importantly, it can eliminate the bit-error rate floor of the conventional optical code-division multiple-access system with the aid of a relatively short spreading code length.

OCIS codes: 060.2605, 200.2605, 010.1330.
doi: 10.3788/COL201210.110603.

Free-space optical (FSO) systems have received considerable attention due to their substantial bandwidth, low power consumption, and high security property[1,2]. The multiple-access interference (MAI) is the primary limitation that will strongly degrade system performance in the multi-user FSO communications[3].

The optical code-division multiple-access (OCDMA) has been developed as a promising candidate for high-rate communications. OCDMA allows multiple users to share the same media simultaneously. The nonzero cross correlation for conventional non-coherent OCDMA systems can cause serious MAI[4]. Long optical orthogonal code (OOC) sequences are required to serve several users simultaneously, resulting in low bandwidth efficiency. Moreover, the complexity of multi-user detection (MUD) is always a serious concern.

A photon-counting-based iterative parallel interference cancellation (Iter-PIC) for the FSO multi-user communications is designed based on the aforementioned scenarios. Each user can be separated by the user-specific interleaver, which avoids the complex design of OOC in OCDMA systems. A log-likelihood ratio (LLR) MAI Iter-PIC algorithm is derived at the receiver, which considers the shot noise, background radiation, and thermal noise. The bit-error rate (BER) performance is evaluated over Gamma-Gamma turbulence-induced fading channels.

The Iter-PIC FSO system structure is shown in Fig. 1. The system employs the on/off key (OOK) modulation and intensity modulated-direct detection technique. Let k be the user index $k \in [1, K]$. The information data $\mathbf{d}_k = \{d_k(l), l = 1, \cdots, L_\mathrm{d}\}$ for kth user is encoded by a forward error correction (FEC) encoder, generating the coded sequence $\mathbf{c}_k = \{c_k(j), j = 1, \cdots, L_\mathrm{c}\}$, where L_d is the information frame length andL_c is the encoded frame length. The encoded data is interleaved by the user-specific interleaver Π_k.

After interleaving, the OOK modulation is employed to produce $\mathrm{x}_k = \{x_k(j), j = 1, \cdots, L_\mathrm{c}\}$. The symbols $\{x_k(j)\}$ are referred to as "chips"[5], which drive an optical modulator for transmission over a FSO link, as shown in Fig. 1(a). The mean photon counts of the transmitted chips are $m_0 = 0$ and $m_1 = \frac{P \cdot T_\mathrm{c}}{h \cdot \upsilon}$ representing "0" and "1" for OOK modulation, where $P, T_\mathrm{c}, \upsilon$, and h are the transmitted power, chip duration, optical frequency, and Plank's constant, respectively.

The Gamma-Gamma turbulence-induced fading is considered. The probability density function (PDF) of channel coefficient I_k is given by[6]

$$f_{I_k}(I_k) = \frac{2(\alpha\beta)^{(\alpha+\beta)/2}}{\Gamma(\alpha)\Gamma(\beta)} I_k^{(\alpha+\beta)/2-1} \mathrm{K}_{\alpha-\beta}\left(2\sqrt{\alpha\beta I_k}\right), \tag{1}$$

where I_k denotes the channel coefficient between the kth user laser and the receiving photon detector (PD). $\alpha > 0$ and $\beta > 0$ are linked to the scintillation index as S.I. $= \alpha^{-1} + \beta^{-1} + (\alpha\beta)^{-1}$. The knowledge of channel coefficient I_k is feasible at the receiver side by channel estimation[7] because of the slow time-varying property of atmospheric turbulence, with correlation time from the order of 10^{-3} seconds to 10^{-2} seconds[8]. Moreover, the channel coefficient remains constant over a number of signal intervals[9].

Ambient light is an important characteristic of the FSO systems. In the context of photon counting, the mean number of ambient photons in the duration of T_c is represented by[3]

$$m_{\mathrm{a,c}} = \frac{\mathrm{W}(\lambda) A \Omega_\mathrm{FOV} \Delta\lambda T_\mathrm{c}}{h\nu}, \tag{2}$$

where Ω_FOV denotes the receiver field of view (FOV), $\Delta\lambda$ is the optical filter bandwidth, and $\mathrm{W}(\lambda)$ is the spectral radiance function.

Figure 1(b) shows that the Iter-PIC receiver consists of a MUD block, noise variance estimation (NVE) block, and K *a posterior* probability (APP) decoders (DECs). Figure 1 shows that the PD is a positive-intrinsic-negative (PIN) diode. The thermal noise and shot noise are considered[3]. The thermal noise current variance of PIN is given by[7–10]

$$\sigma_\mathrm{T}^2 = 4F_\mathrm{n}\Delta f \left(\frac{k_\mathrm{B}T}{R_\mathrm{L}}\right), \tag{3}$$

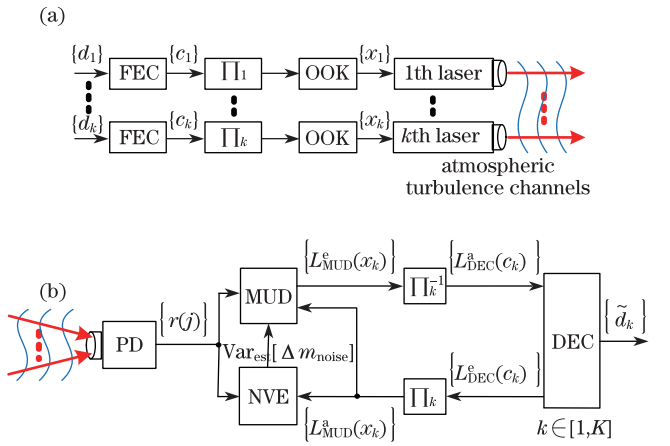

Fig. 1. FSO Iter-PIC system model. (a) transmitter and (b) iterative receiver structures for the kth user.

where k_{B} is the Boltzman's constant, Δf is the PD bandwidth, F_{n} is the amplification factor of the amplifier, and T and R_{L} indicate the absolute temperature and load resistance, respectively.

The PIN shot noise is usually observed as Poisson distribution, and can be approximated by the Gaussian distribution in high energy scenarios[3]. The shot noise variance of each chip duration is represented as

$$\sigma_{\mathrm{S}}^2(j)=2q\left[\sum_{k=1}^{K} i_{\mathrm{p},k}(j)+i_{\mathrm{a,c}}+i_{\mathrm{d}}\right]\Delta f, \tag{4}$$

where i_{d} is the dark current, $i_{\mathrm{a,c}}$ is the current caused by ambient light, q is the electron charge, and $i_{\mathrm{p},k}(j)$ denotes the signal detection current for the kth user. Signal current depends on the received optical power, and can be calculated using the following equation: $i_{\mathrm{p},k}(j)=R\cdot P_k(j)$, where R is the PIN responsiveness and $P_k(j)$ denotes the received optical power of the kth user in the jth chip.

The fluctuating electron counts $\Delta m_{\mathrm{noise}}(j)$ caused by noises can also be modelled after the Gaussian distribution[3] using the following equations:

$$\mathrm{E}\left[\Delta m_{\mathrm{noise}}(j)\right]=0, \tag{5}$$

$$\mathrm{Var}\left[\Delta m_{\mathrm{noise}}(j)\right]=\left[\sigma_{\mathrm{s}}^2(j)+\sigma_{\mathrm{T}}^2\right]\left(\frac{T_{\mathrm{c}}}{q}\right)^2. \tag{6}$$

Moreover, the received optical power of the kth user is written as $P_k(j)=I_k m_k^{\mathrm{Opt}}(j)\,h\upsilon\big/T_{\mathrm{c}}$, where $m_k^{\mathrm{Opt}}(j)$ is the transmitted photon counts of the kth user in the jth chip. In addition, the relation between the responsiveness R and the quantum efficiency η of PIN is $R=\eta\cdot q/h\cdot\upsilon$. Hence, the variance of shot noise is given by

$$\begin{aligned}\sigma_{\mathrm{S}}^2(j)&=2q\left[\sum_{k=1}^{K} i_{\mathrm{p},k}(j)+i_{\mathrm{a,c}}+i_{\mathrm{d}}\right]\Delta f\\&=2q\left[\sum_{k=1}^{K}\eta q I_k m_k^{\mathrm{Opt}}(j)/T_{\mathrm{c}}+\eta q m_{\mathrm{a,c}}/T_{\mathrm{c}}+i_{\mathrm{d}}\right]\Delta f\\&=\left(2q^2\eta\Delta f/T_{\mathrm{c}}\right)\left[\sum_{k=1}^{K} I_k m_k^{\mathrm{Opt}}(j)+m_{\mathrm{a,c}}\right]+2qi_{\mathrm{d}}\Delta f.\end{aligned} \tag{7}$$

The variance of $\Delta m_{\mathrm{noise}}(j)$ is presented as

$$\mathrm{Var}\left[\Delta m_{\mathrm{noise}}(j)\right]=\left(m_{\mathrm{signal}}\sigma_{\mathrm{s},i_{\mathrm{p}}}^2+\sigma_{\mathrm{s},i_{\mathrm{d}}}^2+\sigma_{\mathrm{T}}^2\right)\left(\frac{T_{\mathrm{c}}}{q}\right)^2, \tag{8}$$

where $\sigma_{\mathrm{s},i_{\mathrm{p}}}^2=2q^2\eta\Delta f/T_{\mathrm{c}}$, $\sigma_{\mathrm{s},i_{\mathrm{d}}}^2=2qi_{\mathrm{d}}\Delta f$, and $m_{\mathrm{signal}}=\sum_{k=1}^{K} I_k m_k^{\mathrm{Opt}}(j)+m_{\mathrm{a,c}}$.

The received electron counts can be expressed as

$$r(j)=\eta m_{\mathrm{signal}}+\Delta m_{\mathrm{noise}}(j). \tag{9}$$

A photon-counting-based iteration MUD algorithm is derived. First, the received electron counts are expressed as

$$\begin{aligned}r'(j)&=r(j)-\sum_{k=1}^{K}\eta I_k\frac{m_0+m_1}{2}\\&=\eta\left[\sum_{k=1}^{K} I_k\widetilde{m}_k^{\mathrm{Opt}}(j)+m_{\mathrm{a,c}}\right]+\Delta m_{\mathrm{noise}}(j),\end{aligned} \tag{10}$$

where $\widetilde{m}_k^{\mathrm{Opt}}(j)=m_k^{\mathrm{Opt}}(j)-(m_0+m_1)/2$, $\widetilde{m}_k^{\mathrm{Opt}}(j)=\begin{cases}m_+ & \text{if}\quad x_k(j)=1\\ m_- & \text{if}\quad x_k(j)=0\end{cases}$, $m_+=(m_1-m_0)/2$ and $m_-=-(m_1-m_0)/2$, and $(m_0+m_1)/2$ is the mean of the transmitted photon-counts number per chip.

With *a prior* probability of each chip, the LLR about $x_k(j)$ is defined as

$$L_{\mathrm{MUD}}^{\mathrm{a}}[x_k(j)]=\log\frac{\Pr[\widetilde{m}_k^{\mathrm{Opt}}(j)=m_+]}{\Pr[\widetilde{m}_k^{\mathrm{Opt}}(j)=m_-]}. \tag{11}$$

Thus, $\Pr[\widetilde{m}_k^{\mathrm{Opt}}(j)=m_+]=\frac{\exp[L_{\mathrm{MUD}}^{\mathrm{a}}(x_k(j))]}{1+\exp[L_{\mathrm{MUD}}^{\mathrm{a}}(x_k(j))]}$ and $\Pr[\widetilde{m}_k^{\mathrm{Opt}}(j)=m_-]=\frac{1}{1+\exp[L_{\mathrm{MUD}}^{\mathrm{a}}(x_k(j))]}$.

The estimated mean value and variance of the jth chip electron counts for the kth user are written as

$$\begin{aligned}\mathrm{E}\left[\widetilde{m}_k^{\mathrm{Opt}}(j)\right]&=m_+\Pr\left[\widetilde{m}_k^{\mathrm{Opt}}(j)=m_+\right]\\&\quad+m_-\Pr\left[\widetilde{m}_k^{\mathrm{Opt}}(j)=m_-\right]\\&=\frac{m_+\left\{\exp\left[L_{\mathrm{MUD}}^{\mathrm{a}}(x_k(j))\right]-1\right\}}{1+\exp\left[L_{\mathrm{MUD}}^{\mathrm{a}}(x_k(j))\right]},\end{aligned} \tag{12}$$

$$\begin{aligned}\mathrm{Var}\left[\widetilde{m}_k^{\mathrm{Opt}}(j)\right]&=\left\{m_+-\mathrm{E}\left[\widetilde{m}_k^{\mathrm{Opt}}(j)\right]\right\}^2\\&\quad\cdot\Pr\left[\widetilde{m}_k^{\mathrm{Opt}}(j)=m_+\right]\\&\quad+\left\{m_--\mathrm{E}\left[\widetilde{m}_k^{\mathrm{Opt}}(j)\right]\right\}^2\Pr\left[\widetilde{m}_k^{\mathrm{Opt}}(j)=m_-\right]\\&=m_+^2-\left\{\mathrm{E}\left[\widetilde{m}_k^{\mathrm{Opt}}(j)\right]\right\}^2.\end{aligned} \tag{13}$$

$L^{\mathrm{a}}_{\mathrm{MUD}}(x_k(j)) = 0$ at the first iteration. However, $L^{\mathrm{a}}_{\mathrm{MUD}}(x_k(j))$ is updated by the feedback interleaved LLR $L^{\mathrm{e}}_{\mathrm{DEC}}(c_k(j))$ in the following iterations, as shown in Fig. 1.

Based on Eq. (10), $r'(j)$ can be rewritten as

$$r'(j) = \eta I_k \widetilde{m}_k^{\mathrm{Opt}}(j) + \xi_k(j), \tag{14}$$

where $\xi_k(j)$ is the equivalent noise and $\xi_k(j) = \eta \cdot \sum_{k'=1,k'\neq k}^{K} I_{k'} \widetilde{m}_k^{\mathrm{Opt}}(j) + \Delta m_{\mathrm{noise}}(j)$. Based on the central limit theorem, $\xi_k(j)$ can be approximated by a Gaussian random variable. The mean and variances of $\xi_k(j)$ are expressed as

$$\mathrm{E}[\xi_k(j)] = \mathrm{E}[\Delta m_{\mathrm{noise}}(j)] + \eta \sum_{k'=1,k'\neq k}^{K} I_{k'} \mathrm{E}\left[\widetilde{m}_k^{\mathrm{Opt}}(j)\right], \tag{15}$$

$$\mathrm{Var}[\xi_k(j)] = \eta^2 \sum_{k'=1,k'\neq k}^{K} I_{k'}^2 \mathrm{Var}\left[\widetilde{m}_k^{\mathrm{Opt}}(j)\right] + \mathrm{Var}_{\mathrm{est}}[\Delta m_{\mathrm{noise}}(j)], \tag{16}$$

where

$$\begin{aligned}
&\mathrm{Var}_{\mathrm{est}}[\Delta m_{\mathrm{noise}}(j)] \\
&= \mathrm{E}\left(m_{\mathrm{signal}}\sigma^2_{\mathrm{s},i_{\mathrm{p}}} + \sigma^2_{\mathrm{s},i_{\mathrm{d}}} + \sigma^2_{\mathrm{T}}\right)\left(\frac{T_{\mathrm{c}}}{q}\right)^2 \\
&= \left\{\left\{\sum_{k=1}^{K} I_k \mathrm{E}\left[\widetilde{m}_k^{\mathrm{Opt}}(j)\right] + m_{\mathrm{a,c}}\right\}\sigma^2_{\mathrm{s},i_{\mathrm{p}}} + \sigma^2_{\mathrm{s},i_{\mathrm{d}}} + \sigma^2_{\mathrm{T}}\right\} \\
&\cdot \left(\frac{T_{\mathrm{c}}}{q}\right)^2.
\end{aligned} \tag{17}$$

The MUD block uses modified $\{r'(j)\}$ as its inputs. The corresponding *a posteriori* LLRs about $x_k(j)$ are defined by

$$\begin{aligned}
L[x_k(j)|r'(j)] &= \log\frac{\Pr[r'(j)|x_k(j)=1]}{\Pr[r'(j)|x_k(j)=0]} \\
&\quad + \log\frac{\Pr[x_k(j)=1]}{\Pr[x_k(j)=0]} \\
&= L^{\mathrm{e}}_{\mathrm{MUD}}[x_k(j)] + L^{\mathrm{a}}_{\mathrm{MUD}}[x_k(j)].
\end{aligned} \tag{18}$$

Given the ideal random interleaving or deinterleaving, the output extrinsic LLRs $L^{\mathrm{e}}_{\mathrm{MUD}}(x_k(j))$ is expressed as

$$\begin{aligned}
L^{\mathrm{e}}_{\mathrm{MUD}}[x_k(j)] &= \log\frac{\Pr[r'(j)|x_k(j)=1]}{\Pr[r'(j)|x_k(j)=0]} \\
&= \log\left\{\frac{\frac{1}{\sqrt{2\pi\mathrm{Var}[\xi_k(j)]}}\exp\left\{-\frac{[r'(j)-\eta I_k m_+ - \mathrm{E}(\xi_k(j))]^2}{2\mathrm{Var}(\xi_k(j))}\right\}}{\frac{1}{\sqrt{2\pi\mathrm{Var}[\xi_k(j)]}}\exp\left\{-\frac{[r'(j)-\eta I_k m_- - \mathrm{E}(\xi_k(j))]^2}{2\mathrm{Var}(\xi_k(j))}\right\}}\right\} \\
&= \frac{2\eta I_k m_+ \{r'(j) - \mathrm{E}[\xi_k(j)]\}}{\mathrm{Var}[\xi_k(j)]}.
\end{aligned} \tag{19}$$

Using Eqs. (15) to (17) and (19), the extrinsic LLRs $L^{\mathrm{e}}_{\mathrm{MUD}}(x_k(j))$ can be obtained in the MUD block and transferred to the DEC block after deinterleaving, as shown in Fig. 1.

The APP decoding in the DEC block follows the standard approach[11]. The bit-level LLR $\{L^{\mathrm{bit}}_{\mathrm{DEC}}(d_k(l))\}$ is the sum of the chip-level LLRs $\{L^{\mathrm{a}}_{\mathrm{DEC}}(c_k(j))\}$ when assuming an ideal infinite-length random interleaving or deinterleaving and the independent chips for the specific class of repetition coding, which can be expressed as

$$L^{\mathrm{bit}}_{\mathrm{DEC}}(d_k(l)) = \sum_{j=1}^{L_c} L^{\mathrm{a}}_{\mathrm{DEC}}(c_k((l-1)L_c + j)). \tag{20}$$

The decoding of a repetition code is treated as a linear despreading process. After a hard decision, $\widetilde{d}_k(l) = \left\{\begin{array}{ll} 1 & \text{if } L^{\mathrm{bit}}_{\mathrm{DEC}}(d_k(l)) \geqslant 0 \\ 0 & \text{if } L^{\mathrm{bit}}_{\mathrm{DEC}}(d_k(l)) < 0 \end{array}\right\}$ was used for BER calculation.

The pseudo-code of the Iter-PIC scheme is summarized in Table 1.

Figure 2 reveals that the Iter-PIC algorithm has a fast convergence property. The BER performance greatly improved with increasing number of iterations, converging to a stable state after only five iterations.

Table 1. Algorithm of the Photon-counting-based Iter-PIC

1. Initialization: n=0 and $L^{\mathrm{a}}_{\mathrm{MUD}}\left(x_k^{(n)}(j)\right) = 0$
2. Main Iteration:
2.1) $\mathrm{E}\left[\widetilde{m}_k^{\mathrm{Opt}(n)}(j)\right]$, $\mathrm{Var}\left[\widetilde{m}_k^{\mathrm{Opt}(n)}(j)\right]$, and $Var_{\mathrm{est}}\left[\Delta m^{(n)}_{\mathrm{noise}}(j)\right]$, are calculated in the NVE block using equations (12), (13), and (17), respectively.
2.2) $\mathrm{E}\left[\xi_k^{(n)}(j)\right]$, $\mathrm{Var}\left[\xi_k^{(n)}(j)\right]$, and $L^{\mathrm{e}}_{\mathrm{MUD}}\left[x_k^{(n)}(j)\right]$ are calculated in the MUD block using equations (15), (16), and (19), respectively.
2.3) Deinterleaving and soft APP decoding are preformed.
2.4) After interleaving $L^{\mathrm{a}}_{\mathrm{MUD}}\left[x_k^{(n)}(j)\right]$ is updated.
2.5) If $n \longleftarrow n+1$, go back to step (2.1).
3. After a number of interations, the recovered data $\left[\widetilde{d}_k(j)\right]$ can be obtained and subjected to a hard decision in the DEC block.

Simulations are conducted in this section to evaluate the performance of the Iter-PIC FSO scheme. The simulation parameters are listed in Table 2.

Table 2. Values Used For Numerical Results

Parameter	Value
λ (μm)	1.1
i_{d} (nA)	10
Δf (MHz)	600
T (K)	300
R_{L} (kΩ)	1
F_n	1
Ω_{FOV} (mrad)	5
$\mathrm{W}(\lambda)$ ($\mathrm{W\cdot cm^2\cdot \mu m^{-1}\cdot sr^{-1}}$)	10^{-3}
R responsivity of PIN	0.6

Figure 3 demonstrates that the near single-user performance bound is achievable in the case of four users, indicating that the proposed photon-counting Iter-PIC scheme can be a good candidate for the FSO multi-access method.

Figure 4 shows that the BER floor of the conventional correlator OCDMA system can be eliminated with the Iter-PIC scheme. The Iter-PIC scheme still has better BER performance even with shorter code length (e.g. $R_{\mathrm{C}}^{\mathrm{Rep}}\frac{1}{30},\frac{1}{20}$, which helps improve the system spectral efficiency and is suitable for high-rate FSO communications.

Figure 5 shows that higher S.I. causes severe degradation in BER performance. The performance can be improved by adopting more photon counts per bit in low turbulence channels.

In conclusion, an efficient photon-counting-based Iter-PIC FSO system is proposed. A chip-interleaved iterative MUD algorithm is developed at the receiver. A noise variance estimation method is also designed. The simulations show that the scheme can effectively mitigate the strong multi-user interference with its fast convergence property. The chip-interleaved iterative processing method is useful in high data rate FSO communications.

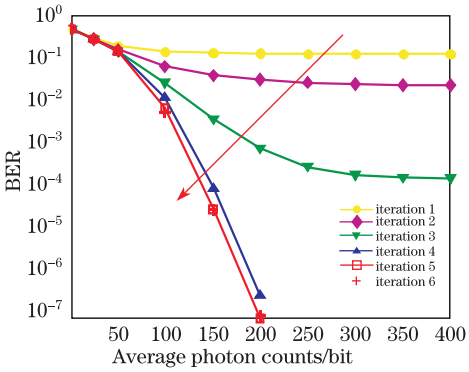

Fig. 2. BER of photon-counting based iterative detection algorithm. $K = 8$ and the repetition FEC coding rate $R^{\mathrm{Rep}} = \frac{1}{10}$.

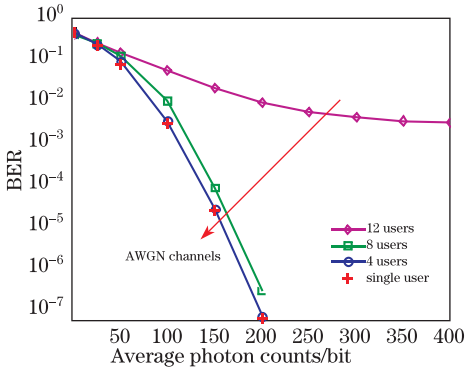

Fig. 3. Impact of user number on the system BER performance. $R^{\mathrm{Rep}} = \frac{1}{10}$.

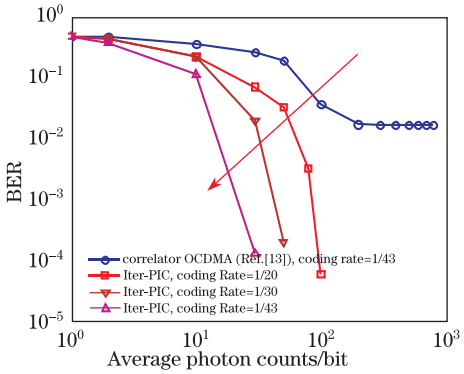

Fig. 4. Comparisons between the Iter-PIC scheme with conventional correlator OCDMA scheme and $K = 7$. OOC is optimal (43, 3, 1) orthogonal code[12].

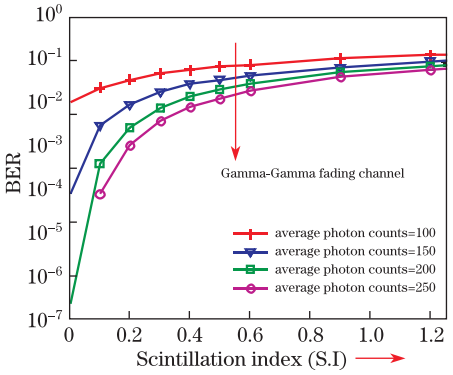

Fig. 5. BER performance over Gamma-Gamma fading channels. $K = 7$ and $R_{\mathrm{C}}^{\mathrm{Rep}} = \frac{1}{10}$

This work was supported by the National Natural Science Foundation of China (No. 60802011) and the National "863" Program of China (No. 2011AA100701).

References

1. V. W. S. Chan, J. Lightwave Technol. **24,** 4750 (2006).
2. C. B. Naila, A. Bekkali, K. Wakamori, and M. Matsumoto, J. Opt. Commun. Netw. **3,** 475 (2011).
3. M. Jazayerifar and J. A. Salehi, IEEE Trans. Commun. **54,** 1614 (2006).
4. H. Shalaby, IEEE Trans. Commun. **50,** 2009 (2002).
5. Li Ping, L. Liu, K. Y. Wu, and W. K. Leung, IEEE Trans. Wireless Commun. **5,** 938 (2006).
6. T. Miyazawa and I. Sasase, J. Lightwave Technol. **25,** 2992 (2007).
7. I. B. Djordjevic, J. Lightwave Technol. **2,** 221 (2010).
8. A. A. Farid, IEEE Trans. Commun. **60,** 479 (2012).
9. M. Cole and K. Kiasaleh, IEEE Trans. Commun. **55,** 2341 (2007).
10. G. P. Agrawal, *Fiber Optic Communication Systems* (Wiley, Hoboken, 2002) chap. 6, p. 348.
11. C. Berrou and A. Glavieux, IEEE Trans. Commun. **44,** 1261 (1996).
12. F. R. K. Chung, J. A. Salehi, and V. K. Wei, IEEE Trans. Inf. Theory **35,** 595 (1989).